KINETIC TRANSFORMATION OF SPINEL TYPE $LiMn_2O_4$ INTO TUNNEL TYPE MnO_2

Daud K. Walanda

Chemistry Department, Faculty of Education, Universitas Tadulako, Palu 94118, Indonesia

Received 17 April 2007; Accepted 6 June 2007

ABSTRACT

Lithiated phase $LiMn_2O_4$ is a potential cathode material for high-energy batteries because it can be used in conjunction with suitable carbon anode materials to produce so-called lithium ion cells. The kinetic transformation of $LiMn_2O_4$ into manganese dioxide (MnO_2) in sulphuric acid has been studied. It is assumed that the conversion of $LiMn_2O_4$ into R-MnO_2 is a first order autocatalytic reaction. The transformation actually proceeds through the spinel λ-MnO_2 as an intermediate species which is then converted into gamma phase of manganese dioxide. In this reaction $LiMn_2O_4$ whose structure spinel type, which is packing between tetrahedral coordination and octahedral coordination, is converted to form octahedral tunnel structure of manganese dioxide, which is probably regarded as a reconstructive octahedral-coordination transformation. Therefore, it is a desire to investigate the transformation of manganese oxides in solid state chemistry by analysing XRD powder patterns. Due to the reactions involving solids, concentrations of reactant and product are approached with the expression of peak areas.

Keywords: *high-energy battery, lithium ion cells, kinetic transformation*

INTRODUCTION

Among the many materials investigated as potential cathode materials for high-energy batteries, manganese oxides remain potentially attractive compared to cobalt based materials because of their low cost and toxicity, and added safety on overcharge [1]. The lithiated phase $LiMn_2O_4$ is of particular interest because it can be used in conjunction with suitable carbon anode materials to produce the so-called lithium ion (Li-ion) or "rocking chair" cells [2]. $LiMn_2O_4$ does not have a layered crystal structure but a spinel structure, which has three-dimensional channels allowing lithium insertion within the $Mn^{3+/4+}$ redox couple and hence has large electrochemical capacity in the 4 V region [3].

Thackeray *et al.* [3, 4] have contributed substantially to highlighting the implications of the structural features of $LiMn_2O_4$ on its electrochemical behaviour. This spinel oxide has lithium ions residing in tetrahedral (8a) sites, the manganese ions in octahedral (16d) sites and O^{2-} ions in octahedral (32e) sites, which therefore can be assigned as $(Li)_{8a}[Mn^{III}Mn^{IV}]_{16d}O_4$. Nevertheless, $LiMn_2O_4$ still suffers from some major problems including (i) a low specific capacity associated with a low density compared to other cathode materials; (ii) a potentially lower power than the layered materials ($LiCoO_2$ and $LiNiO_2$); and (iii) fading and losses on storage capability are very high particularly at increased temperature [5]. The irreversible capacity loss is ascribed to several factors, namely; (i) an electrochemical decomposition of the electrolyte solution; (ii) a slow dissolution of manganese from the active cathode into the electrolyte; (iii) structural instability, and; (iv) the Jahn-Teller effect resulting in phase degradation, especially in deeply discharge $LiMn_2O_4$ [6]. Improvements to the electrochemical performance of the spinel have been demonstrated by a number of group such as Ohzuku *et al.* [7], Tarascon *et al.* [8] and Guyomard and Tarascon [9], who have reported the dependency of the electrochemical performance of $LiMn_2O_4$ on the conditions of synthesis. Moreover, Yamane *et al.* [10] have found that capacity fading during storage and cycling are related to each other. Pistoia *et al.* [11, 12] have investigated the influence of electrolyte, current collector, voltage range and cathodic additives on the capacity loss of lithium manganese oxides, and also that of the preparative conditions.

$LiMn_2O_4$ is usually synthesised by the classical solid state route (the ceramic procedure) using mixtures of several manganese and lithium sources heated in air at high temperatures (between 600 and 900 ^oC [13-15]) with slow cooling of the furnace. The sample obtained at about 750 ^oC shows the best electrochemical performance [13]. This method has the advantages of low cost of production and high productivity; however, less compositional homogeneity is apparent including by-products, strong aggregation and important particle distribution restrict its applicability for advanced ceramics [16]. Recently, various preparative techniques have been developed which are based on the processes of co-precipitation, ion-exchange or thermal decomposition at low temperature [17].

In terms of the reactivity of the Li-Mn-O system in acidic media, Vol'khin *et al.* [18, 19] first reported that a spinel-type manganese oxide without metal ions in the tunnel can be obtained by extracting lithium ion from a

* Email address: walanda@gmail.com

spinel-type lithium manganese with an acid. Years later, Hunter [20] described the structural relationship between the spinel $LiMn_2O_4$ and the lithium deficient materials with general formula as $Li_{1-x}Mn_2O_4$. The author discovered that acid treatment of the spinel $LiMn_2O_4$ yielded λ-MnO_2 according to the disproportionation reaction:

$$2LiMn_2O_4 \longrightarrow 3\lambda\text{-}MnO_2 + MnO + Li_2O \quad (1)$$

in which MnO and LiO_2 were leached from the parent structure. According to Hunter [20], the reaction involves a surface disproportionation mechanism in which the disproportionation of Mn(III) into Mn(IV) and Mn(II) coupled with electron hopping from the bulk to the surface, and dissolution of soluble Mn(II) and lithium ions from the surface, instead of one involving an ion exchange for the topotactic extraction of lithium from the $LiMn_2O_4$ with acid.

The phase transformation between $LiMn_2O_4$ and R-MnO_2 as well as β-MnO_2 has been studied by Thackeray [21] who reported that upon heating under inert conditions, such as under vacuum, the lithiated R-MnO_2 transforms readily into the spinel $LiMn_2O_4$ at 300 ^oC. Whereas, heating in air leads to $LiMn_2O_{4.5}$. The author has also proposed the model of the tunnel R-MnO_2 to spinel transformation, which involves an initial shear of the oxygen array to close cubic-packing and a displacement of 50 % of the manganese ions into neighbouring interstitial octahedra.

EXPERIMENTAL SECTION

$LiMn_2O_4$ was prepared by thoroughly mixing appropriate molar ratios of Li_2CO_3 (Merck) and Mn_2O_3 powders by hand with pestle in a mortar and the reagents were heated in a furnace at 750 ^oC and then allowed to cool freely in the furnace. The reaction occurred in this is:

$$Li_2CO_3 + 2Mn_2O_3 + \tfrac{1}{2}O_2 \rightarrow 2LiMn_2O_4 + CO_2 \quad (2)$$

A kinetic study of $LiMn_2O_4$ decomposition was conducted by which 10 g of $LiMn_2O_4$ was digested in sulphuric acid with concentrations of either 0.5, 1.0 or 2.0 M.

X-Ray Diffraction Analysis

X-ray diffraction analysis of each sample was conducted at room temperature using a Philips 1710 diffractometer with Cu K_α radiation of wavelength 1.5891 Å. The instrumental conditions that were employed as follows:

(a) X-ray generator settings of 40 kV and 30 mA.
(b) A scan range of 10 – 80 $^o2\theta$
(c) A step size of 0.05 $^o2\theta$ every 2.5 seconds
(d) A divergence slit width of 1^o
(e) A receiving slit 0.1 mm

Samples were mounted by a backfilling procedure in flat aluminium holders.

Peak Parameters

The peak parameters including the peak width at half height, more commonly called full width at half maximum (FWHM), the peak position and the maximum intensity were determined by fitting a Lorentzian lineshape (Eqn 3.9) [22] of the XRD experimental data using "Solver" function in an appropriate Microsoft Excel spreadsheet. That is,

$$I = I_{MAX}\frac{W^2}{4[(W/2)^2 + (X - \mu)^2]} \quad (3)$$

where W is the peak width at half height or FWHM, I_{MAX} is the maximum intensity of the peak and μ is the peak position. A linear background was also assumed during the fitting process.

RESULTS AND DISCUSSION

The digestion of $LiMn_2O_4$ in H_2SO_4 solutions is believed to occur via the following reactions:

$$LiMn_2O_4 \rightarrow 2MnO_2 + Li^+ + e^- \quad (4)$$

$$LiMn_2O_4 + 4H^+ + e^- \rightarrow 2MnO_2 + Mn^{2+} + Li^+ + 2H_2O \quad (5)$$

and the overall reaction is:

$$2LiMn_2O_4 + 4H^+ \rightarrow 3MnO_2 + Mn^{2+} + 2Li^+ + 2H_2O \quad (6)$$

Therefore, adapting the mechanism found in the corresponding Mn_2O_3 [23] the mechanism of digestion of $LiMn_2O_4$ in H_2SO_4 involves three steps:

$$\begin{matrix} LiMn_2O_4 \xrightarrow{\text{Li-extraction}} \lambda - MnO_2 \xrightarrow{\text{dissolution}} \\ Mn(III) \xrightarrow{\text{dispropotionation-precipitation}} \text{Manganese Dioxide} \end{matrix} \quad (7)$$

Larcher *et al.* [24] have studied acid digestion of $LiMn_2O_4$ in 2.5 M sulfuric acid at various temperatures and time in which they observed various phases of manganese dioxide such as γ-MnO_2 and α-MnO_2. In addition, they reported that the mechanism of $\lambda \rightarrow \alpha/\gamma$ transition was found to be the result of a dissolution-crystallisation mechanism.

In this study, the process of lithium-extraction from $LiMn_2O_4$ occurred at around 0.5M acid concentration, and the conversion of the λ-MnO_2 spinel structure by acid into tunnel structure of manganese dioxide such as R-MnO_2 and β-MnO_2 starts at a temperature of 60 ^oC. This inter-conversion between manganese dioxides is interesting in terms of our structural study. The ramsdellite is a major phase of manganese dioxide observed in this study which is formed over the acid concentration range 0.5 and 5.0

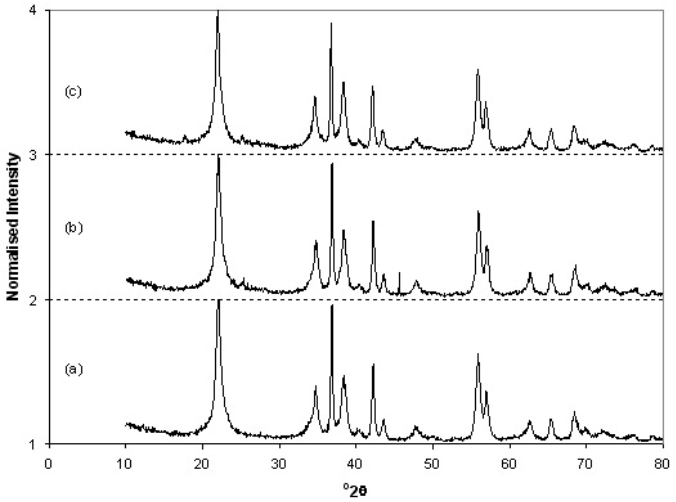

Fig 1. XRD patterns of sample produced from acid digestion of different [H_2SO_4] (**a**) 2.0M, (**b**) 2.5M and (**c**) 3.0M.

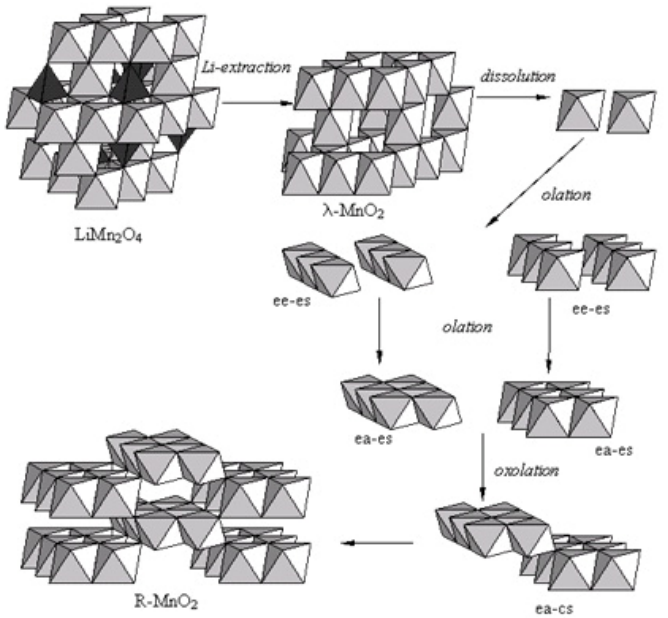

Fig 2. Possible reaction mechanism of the formation of R-MnO_2 during acid digestion of $LiMn_2O_4$.

M. The effect of acid concentration in preparing R-MnO_2 was studied by digesting $LiMn_2O_4$ in 2.0, 2.5 and 3.0 M H_2SO_4 for 48 h at 98 °C.

As shown in Fig 1, in 2.0M the products observed were mainly pure R-MnO_2, whereas in 2.5M and 3.0M small amount of α-MnO_2 present in the mixture. This information is valuable for application in kinetic studies in which the $LiMn_2O_4$ transform into single phase of R-MnO_2.

Upon digestion, the manganese aquo-hydroxo cations experience condensation reactions through olation and oxolation to form several types of manganese dioxide via (i) an equatorial-equatorial edge-sharing (ee-ss) linkage, (ii) an equatorial-axial edge-sharing (ea-ss) linkage and (iii) an equatorial-axial corner-sharing (ea-cs) linkage of the octahedral [23]. Formation of R-MnO_2 probably occurs from the polycondensation of the aqua-hydroxo ions by an equatorial-equatorial edge-sharing linkage of the octahedral monomer forming a continuous array and followed by the equatorial-axial edge-sharing linkage of the octahedra arrays forming a growth unit for R-MnO_2 as shown in the Fig 2. The formation of R-MnO_2 subsequently took place via an equatorial-axial corner-sharing linkage which precipitates to form the manganese dioxide.

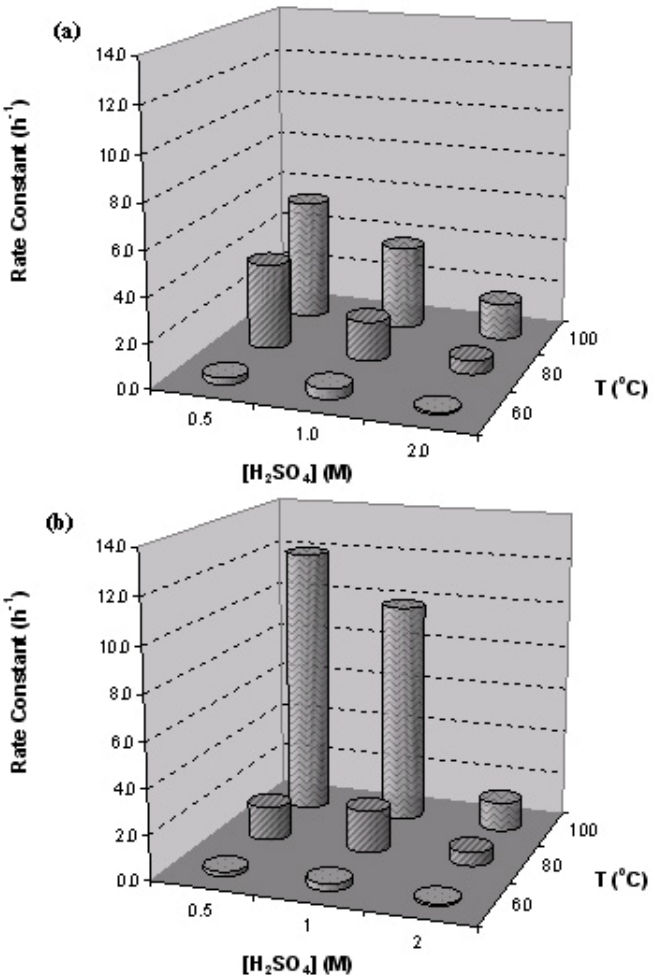

Fig 3. Kinetic rate of (a) $LiMn_2O_4$ disappearance and (b) MnO_2 formation.

Kinetic Study

Transformation of $LiMn_2O_4$ by acid digestion into ramsdellite-manganese dioxide actually proceeds through the spinel λ-MnO_2 as an intermediate species. However, it is assumed that the conversion of $LiMn_2O_4$ into R-MnO_2 is a first order autocatalytic reaction, since

Table 1. Activation Energies of $LiMn_2O_4$ Disappearance and MnO_2 Formation.

$[H_2SO_4]$ (M)	$LiMn_2O_4$ Disappearance E_a ($kJmol^{-1}$)	R-MnO_2 Formation E_a ($kJmol^{-1}$)
0.5	-9.0	-12.5
1.0	-6.6	-10.7
2.0	-9.1	-7.9

the kinetic curve profile being similar to the Mn_2O_3 [25] transformation. Therefore in this case Eqn (8) is applied to generate the kinetic rate of the conversion.

$$x = \frac{X_B(e^{kt} - 1)}{1 + be^{kt}} \qquad (8)$$

As shown in Fig 3 at temperatures of 60 ^oC and 80 ^oC the transformation rate of $LiMn_2O_4$ disappearance is higher than that of R-MnO_2 formation. At 100 ^oC the situation is even more extreme with the rate of $LiMn_2O_4$ being twice that of R-MnO_2 formation. In addition, the transformation rate of both $LiMn_2O_4$ disappearance and R-MnO_2 formation are decreased as the acid is increased. This phenomenon is contrary to the corresponding Mn_2O_3. A possible explanation for this trend is that upon acid digestion of $LiMn_2O_4$ the favoured product is R-MnO_2 rather than γ-MnO_2 which consists of a micro-scale intergrowth of the ramsdellite and pyrolusite. Since the γ-MnO_2 contain pyrolusite site, the structure have less an equatorial-axial edge-sharing (ea-es) linkage (as shown in the Fig 2) compare to the R-MnO_2. Therefore, the formation rate of R-MnO_2 is slow because of the time needed for another equatorial-axial edge-sharing (ea-es) linkage.

CONCLUSION

The activation energy of the above kinetic transformations has been determined (Table 1) and that there is a trend with acid concentration for R-MnO_2 formation; however, it is not seen with $LiMn_2O_4$ disappearance. This could mean that both disappearance and formation reactions undergo different mechanisms.

REFERENCES

1. Ammundsen, B. and Paulsen, J., 2001, *Adv. Mater.*, 13, 943.
2. Reimers, J. N., Dahn, J. R. and von Sacken, U., 1993, *J. Electrochem. Soc.*, 140, 2752.
3. Thackeray, M. M., Johnson, P. J., de Picciotto, L. A., Bruce, P. G. and Goodenough, J. B., 1984, *Mater. Res. Bull.*, 19, 179.
4. Thackeray, M. M., David, W. I. F., Bruce, P. G. and Goodenough, J. B., 1983, *Mater. Res. Bull.*, 18, 461.
5. Broussely, M., Biensan, P. and Simon, B., 1999, *Electrochim. Acta*, 45, 3.
6. Huang, H., Chen, C. H., Perego, R. C., Kelder, E. M., Chen, L., Schoonman, J., Weydanz, W. J. and Nielsen, D. W., 2000, *Solid State Ionics*, 127, 31.
7. Ohzuku, T., Kitagawa, M. and Hirai, T., 1990, *J. Electrochem. Soc.*, 137, 769.
8. Tarascon, J. M., Wang, E., Shokoohi, F. K., McKinnon, W. R. and Colson, S., 1991, *J. Electrochem. Soc.*, 138, 2859.
9. Guyomard, D. and Tarascon, J. M., 1994, *Solid State Ionics*, 69, 222.
10. Yamane, H., Saitoh, M., Sano, M., Fujita, M., Sakata, M., Takada, M., Nishibori, E. and Tanaka, N., 2002, *J. Electrochem. Soc.*, 149, A1514.
11. Pistoia, G., Antonini, A., Rosati, R. and Zane, D., 1996, *Electrochimica Acta*, 41, 2683.
12. Antonini, A., Bellitto, C., Pasquali, M. and Pistoia, G., 1998, *J. Electrochem. Soc.*, 145, 2726.
13. Manev, V., Banov, B., Momchilov, A. and Nassalevska, A., 1995, *J. Power Sources*, 57, 99.
14. Thackeray, M. M. and Rossouw, M. H., 1994, *J. Solid State Chem.*, 113, 441.
15. Gao, Y. and Dahn, J. R., 1996, *J. Electrochem. Soc.*, 143, 100.
16. Nakamura, T. and Kajiyama, A., 1999,*Solid State Ionics*, 124, 45.
17. Wu, H. M., Tu, J. P., Yuan, Y. F., Li, Y., Zhao, X. B. and Cao, G. S., 2005, *Mater. Sci. & Eng. B: Solid-State Mater. Adv. Techn.*, 119, 75.
18. Leont'eva, G. V. and Vol'khin, V. V., 1971, *Zhurnal Prikladnoi Khimii (S. -Peterburg)*, 44, 2615.
19. Vol'khin, V. V., Leont'eva, G. V. and Onorin, S. A., 1973, *Neorganicheskie Materialy*, 9, 1041.
20. Hunter, J. C., 1981, *J. Solid State Chem.*, 39, 142.
21. Thackeray, M. M., 1997, *Prog. Solid State Chem.*, 25, 1.
22. Donne, S. W., 1996, *PhD Thesis*, Newcastle University, Newcastle, Australia.
23. Walanda, D. K., Lawrance, G. A. and Donne, S. W., 2005, *J. Power Sources*, 139, 325.
24. Larcher, D., Courjal, P., Urbina, R. H., Gerand, B., Blyr, A., Du Pasquier, A. and Tarascon, J. M., 1998, *J. Electrochem. Soc.*, 145, 3392.
25. Walanda, D. K., 2006, *PhD Thesis*, The University of Newcastle, Newcastle, Australia.